Optics Letters

Comprehensive vector analysis for electro-optical, opto-electronic, and optical devices

TING QING, SHUPENG LI, XIAOHU TANG, PING LI, XUFENG CHEN, LIHAN WANG, YIJIE FANG, MEIHUI CAO, LUGANG WU, AND SHILONG PAN*

Key Laboratory of Radar Imaging and Microwave Photonics, Ministry of Education, Nanjing University of Aeronautics and Astronautics, Nanjing 210016, China
**Corresponding author: pans@nuaa.edu.cn*

Received 17 February 2021; revised 14 March 2021; accepted 14 March 2021; posted 16 March 2021 (Doc. ID 422817); published 6 April 2021

High-performance electro-optical (E-O), opto-electronic (O-E), and optical (O-O) devices are widely used in optical communications, microwave photonics, fiber sensors, and so on. Measurement of the amplitude and phase responses are essential for the development and fabrication of these devices. However, the previous methods can hardly characterize the E-O, O-E, and O-O devices with arbitrary responses. Here we propose a comprehensive vector analyzer based on optical asymmetrical double-sideband (ADSB) modulation to overcome this difficulty. The ADSB solves the problem of frequency aliasing and can extract information from both the +1st- and −1st-order sidebands. Thus, most devices in photonic applications, including phase modulators, can be characterized. In the experiment, a commercial photodetector, a phase modulator, and a sampled FBG are used as the O-E, E-O, and O-O devices under test, respectively. A frequency resolution of 2 MHz, an electrical sweeping range of 40 GHz, and an optical sweeping range of 80 GHz are achieved.

https://doi.org/10.1364/OL.422817

Electro-optical (E-O), opto-electronic (O-E), and optical (O-O) devices, such as modulators, photodetectors (PDs), and optical filters, play key roles in optical communication [1], microwave photonics [2], and optical instrumentation [3]. Measurement of their frequency responses is essential in the application and fabrication of these devices, because almost all the important parameters, such as half-wave voltage and modulation index of the E-O devices, 3 dB bandwidth, and responsivity of the O-E devices and insertion loss, group delay, and chromatic dispersion of the O-O devices, can be derived from the frequency responses. In general, a lightwave component analyzer (LCA) can be employed to characterize E-O, O-E, and O-O devices [4,5]. However, by utilizing the double-sideband (DSB) modulation, commercial LCAs cannot measure the E-O and O-O devices with arbitrary responses, such as phase modulators and fiber Bragg gratings (FBGs). This is because, in DSB-based measurement, the two first-order sidebands are beaten with the optical carrier in the PD and generate RF signals with the same frequencies, resulting in frequency aliasing [6]. When measuring phase modulators, the frequency responses carried by the two first-order sidebands with opposite phases cancel out after photodetection, making the LCA unable to directly detect the phase-modulated signal. When measuring O-O devices, the LCA employs intensity-modulated signals to measure O-O devices such as FBGs. The frequency responses carried by the two first-order sidebands would be superimposed after photodetection and difficult to differentiate.

To characterize E-O devices with arbitrary responses, a few methods based on an optical spectrum analyzer (OSA) [7] and interferometry [8] are proposed. However, the OSA-based method has a poor resolution (typically several gigahertz), and the interferometry method is easily affected by mechanical vibration and thermal fluctuations. To overcome these problems, methods based on two-tone modulation [9] and phase modulation to intensity modulation conversion [10] are proposed. However, the two methods require complicated systems.

To measure O-O devices with arbitrary responses, methods based on modulation phase shift [11] and interferometry [12] can be applied. However, both methods have a relatively low resolution (typically hundreds of megahertz) due to the poor wavelength repeatability of tunable laser sources. Recently, methods based on multi-frequency modulation [13], optical single-sideband modulation [14,15], and linear-frequency modulation [16] have been proposed to improve the resolution (sub-megahertz to several megahertz), but the dynamic range is relatively low (20–60 dB).

In this Letter, we propose a comprehensive vector analyzer (CVA) for accurate measurement of E-O, O-E, and O-O devices with arbitrary responses. By employing the optical asymmetrical double-sideband (ADSB) modulation [6,17–20], the frequency response of a phase modulator can be transferred into a frequency-shifted photocurrent, and the frequency responses carried by the ±1st-order sidebands, respectively, can be extracted. In addition, the measurement errors introduced by the modulation nonlinearity can be removed by the ADSB structure, leading to a large dynamic range (e.g., 90 dB

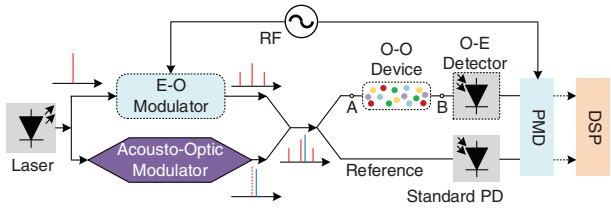

Fig. 1. Schematic diagram of the CVA for E-O, O-E, and O-O devices. RF, radio frequency; PD, photodetector; PMD, phase-magnitude detector; DSP, digital signal processor.

in [17] for O-O device measurement). The fine frequency sweeping of the microwave source also enables a high resolution (e.g., 334 Hz in [17]). To evaluate the proposed CVA, proof-of-concept experiments are performed. A PD (O-E device), a phase modulator (E-O device), and a sampled FBG (O-O device) are measured. Compared with previous methods, the proposed CVA is a universal measurement method for E-O, O-E, and O-O devices with arbitrary responses.

The schematic diagram of the CVA is shown in Fig. 1. An optical carrier at ω_o is launched by a laser and then divided into two branches. In the E-O branch, the optical signal is modulated by a sweeping RF signal at an E-O modulator and generates an optical double-sideband (ODSB) modulation signal. The ODSB signal can be written as

$$\begin{aligned} E_{\mathrm{ODSB}}(\omega) = {} & a\,H_{\mathrm{EO}}(\omega_{\mathrm{o}}-\omega_{\mathrm{e}})\delta\left[\omega-(\omega_{\mathrm{o}}-\omega_{\mathrm{e}})\right] \\ & + a\,H_{\mathrm{EO}}(\omega_{\mathrm{o}}+\omega_{\mathrm{e}})\delta\left[\omega-(\omega_{\mathrm{o}}+\omega_{\mathrm{e}})\right] \\ & + a\,H_{\mathrm{EO}}(\omega_{\mathrm{o}})\delta(\omega-\omega_{\mathrm{o}}), \end{aligned} \tag{1}$$

where ω_e is the angular frequency of the RF signal, a is the complex amplitude of the carrier of the ODSB signal, and $H_{\mathrm{EO}}(\omega)$ is the frequency response of the E-O modulator.

In the other branch, the optical signal is frequency-shifted in an acousto-optic modulator (AOM). The frequency shift is $\Delta\omega$, and the complex amplitude is b. The combined signal of the ODSB signal and the frequency-shifted carrier is called the ADSB signal, which can be expressed as

$$\begin{aligned} E_{\mathrm{ADSB}}(\omega) = {} & a\,H_{\mathrm{EO}}(\omega_{\mathrm{o}}-\omega_{\mathrm{e}})\delta\left[\omega-(\omega_{\mathrm{o}}-\omega_{\mathrm{e}})\right] \\ & + a\,H_{\mathrm{EO}}(\omega_{\mathrm{o}}+\omega_{\mathrm{e}})\delta\left[\omega-(\omega_{\mathrm{o}}+\omega_{\mathrm{e}})\right] \\ & + a\,H_{\mathrm{EO}}(\omega_{\mathrm{o}})\delta(\omega-\omega_{\mathrm{o}}) + b\delta\left[\omega-(\omega_{\mathrm{o}}+\Delta\omega)\right]. \end{aligned} \tag{2}$$

Since the phase difference of a and b is a constant, it can be ignored. The absolute value of a and b can be measured by an optical power meter.

The ADSB signal is divided into the reference branch and the measurement branch. In the reference branch, the ADSB signal is directly injected into a standard PD.

The frequency response of the standard PD, i.e., $H_{\mathrm{std}}(\omega)$, is previously calibrated, which will be used as a reference. After square-law detection of the standard PD, the AC terms of the generated photocurrent are

$$\begin{aligned} i_{\mathrm{std}}(\omega_{\mathrm{e}}-\Delta\omega) &= a b^{*} H_{\mathrm{EO}}(\omega_{\mathrm{o}}+\omega_{\mathrm{e}})\,H_{\mathrm{std}}(\omega_{\mathrm{e}}-\Delta\omega) \\ i_{\mathrm{std}}(\omega_{\mathrm{e}}+\Delta\omega) &= a^{*} b\,H_{\mathrm{EO}}^{*}(\omega_{\mathrm{o}}-\omega_{\mathrm{e}})\,H_{\mathrm{std}}(\omega_{\mathrm{e}}+\Delta\omega). \end{aligned} \tag{3}$$

The magnitude and phase information are extracted by a phase-magnitude detector (PMD). Since $H_{\mathrm{std}}(\omega)$ is known, $H_{\mathrm{EO}}(\omega)$ can be obtained as

$$\begin{aligned} H_{\mathrm{EO}}(\omega_{\mathrm{o}}+\omega_{\mathrm{e}}) &= \frac{i_{\mathrm{std}}(\omega_{\mathrm{e}}-\Delta\omega)}{a b^{*} H_{\mathrm{std}}(\omega_{\mathrm{e}}-\Delta\omega)} \\ H_{\mathrm{EO}}(\omega_{\mathrm{o}}-\omega_{\mathrm{e}}) &= \left[\frac{i_{\mathrm{std}}(\omega_{\mathrm{e}}+\Delta\omega)}{a^{*} b\,H_{\mathrm{std}}(\omega_{\mathrm{e}}+\Delta\omega)}\right]^{*}. \end{aligned} \tag{4}$$

As can be seen in (4), the frequency responses of the E-O modulator in both ±1st sidebands can be measured, which indicates that the CVA can characterize the phase modulators.

To measure the frequency response of the O-E detector, the O-O device is removed, and the A port and B port are directly connected. In the measurement branch, the ADSB signal is sent to the O-E detector. After square-law detection of the O-E detector, the output signals are

$$\begin{aligned} i_{\mathrm{OE}}(\omega_{\mathrm{e}}-\Delta\omega) &= a b^{*} H_{\mathrm{EO}}(\omega_{\mathrm{o}}+\omega_{\mathrm{e}})\,H_{\mathrm{OE}}(\omega_{\mathrm{e}}-\Delta\omega) \\ i_{\mathrm{OE}}(\omega_{\mathrm{e}}+\Delta\omega) &= a^{*} b\,H_{\mathrm{EO}}^{*}(\omega_{\mathrm{o}}-\omega_{\mathrm{e}})\,H_{\mathrm{OE}}(\omega_{\mathrm{e}}+\Delta\omega), \end{aligned} \tag{5}$$

where $H_{\mathrm{OE}}(\omega)$ is the frequency response of the O-E detector. Since $H_{\mathrm{EO}}(\omega)$ is obtained in (4), $H_{\mathrm{OE}}(\omega)$ can be derived from one of the equations in (5), i.e.,

$$\begin{aligned} H_{\mathrm{OE}}(\omega_{\mathrm{e}}-\Delta\omega) &= \frac{i_{\mathrm{OE}}(\omega_{\mathrm{e}}-\Delta\omega)}{a b^{*} H_{\mathrm{EO}}(\omega_{\mathrm{o}}+\omega_{\mathrm{e}})} \\ H_{\mathrm{OE}}(\omega_{\mathrm{e}}+\Delta\omega) &= \left[\frac{i_{\mathrm{OE}}(\omega_{\mathrm{e}}+\Delta\omega)}{a b^{*} H_{\mathrm{EO}}(\omega_{\mathrm{o}}-\omega_{\mathrm{e}})}\right]^{*}. \end{aligned} \tag{6}$$

To characterize the O-O device, the ADSB signal undergoes the O-O device and then enters into the O-E detector. The output photocurrent can be written as

$$\begin{aligned} i_{\mathrm{OO}}(\omega_{\mathrm{e}}-\Delta\omega) = {} & a b^{*} H_{\mathrm{EO}}(\omega_{\mathrm{o}}+\omega_{\mathrm{e}})\,H_{\mathrm{OE}}(\omega_{\mathrm{e}}-\Delta\omega) \\ & \cdot H_{\mathrm{OO}}(\omega_{\mathrm{o}}+\omega_{\mathrm{e}})\,H_{\mathrm{OO}}^{*}(\omega_{\mathrm{o}}+\Delta\omega) \\ i_{\mathrm{OO}}(\omega_{\mathrm{e}}+\Delta\omega) = {} & a^{*} b\,H_{\mathrm{EO}}^{*}(\omega_{\mathrm{o}}-\omega_{\mathrm{e}})\,H_{\mathrm{OE}}(\omega_{\mathrm{e}}+\Delta\omega) \\ & \cdot H_{\mathrm{OO}}^{*}(\omega_{\mathrm{o}}-\omega_{\mathrm{e}})\,H_{\mathrm{OO}}(\omega_{\mathrm{o}}+\Delta\omega), \end{aligned} \tag{7}$$

where $H_{\mathrm{OO}}(\omega)$ is the frequency response of the O-O device. Since $H_{\mathrm{EO}}(\omega)$ and $H_{\mathrm{OE}}(\omega)$ are obtained in (4) and (6), and $H_{OO}(\omega_O+\Delta\omega)$ is a measureable constant, the frequency response of the O-O device can be derived as

$$\begin{aligned} & H_{\mathrm{OO}}(\omega_{\mathrm{o}}+\omega_{\mathrm{e}}) \\ & = \frac{i_{\mathrm{OO}}(\omega_{\mathrm{e}}-\Delta\omega)}{a b^{*} H_{\mathrm{EO}}(\omega_{\mathrm{o}}+\omega_{\mathrm{e}})\,H_{\mathrm{OE}}(\omega_{\mathrm{e}}-\Delta\omega)\,H_{\mathrm{OO}}^{*}(\omega_{\mathrm{o}}+\Delta\omega)} \\ & H_{\mathrm{OO}}(\omega_{\mathrm{o}}-\omega_{\mathrm{e}}) \\ & = \left[\frac{i_{\mathrm{OO}}(\omega_{\mathrm{e}}+\Delta\omega)}{a^{*} b\,H_{\mathrm{EO}}^{*}(\omega_{\mathrm{o}}-\omega_{\mathrm{e}})\,H_{\mathrm{OE}}(\omega_{\mathrm{e}}+\Delta\omega)\,H_{\mathrm{OO}}(\omega_{\mathrm{o}}+\Delta\omega)}\right]^{*}. \end{aligned} \tag{8}$$

The calculations of (4), (6), and (8) are performed by a digital signal processor (DSP). It is worth noting that the frequency response of the E-O modulator and O-E detector can

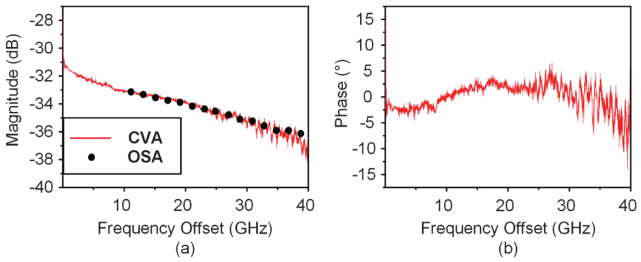

Fig. 2. Measured (a) magnitude and (b) phase responses of the phase modulator by using the proposed CVA.

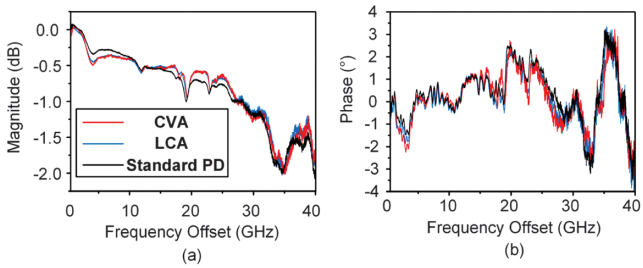

Fig. 3. (a) Normalized magnitude and (b) phase responses of the standard PD and the PD under test. The PD under test is measured by the proposed CVA and an LCA.

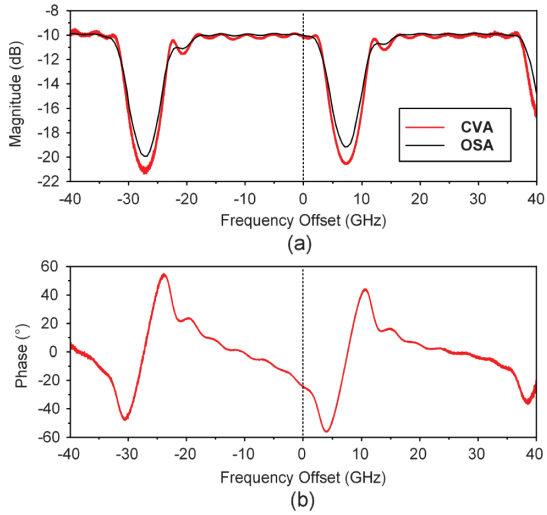

Fig. 4. Measured (a) magnitude and (b) phase responses of the sampled FBG by using the proposed CVA.

be removed through direct calibration [6,17–19] in the measurement of the O-O device. Sweeping the frequency of the RF signal, the frequency response of the E-O, O-E, and O-O devices are obtained according to (4), (6), and (8).

Experiments are performed based on the configuration in Fig. 1. The optical carrier is generated by a tunable laser source (Agilent N7714A) with a linewidth of 100 kHz, which is split into two branches through an optical coupler. A modulator under test is placed in the E-O branch, which can be any E-O modulator, such as Mach–Zehnder modulator, phase modulator, and polarization modulator. In this experiment, a phase modulator (EOSPACE, Inc.) is employed as the modulator under test. In the other branch, an AOM (Gooch & Housego, Inc.) shifts the frequency of the optical carrier by 80 MHz. The modulated signal and frequency-shifted signal are combined, and the power is divided by an optical coupler. A sampled FBG is used as the O-O device under test. Two PDs (Finisar XPDV2120RA) with a bandwidth of 40 GHz are exploited as the O-E detector under test and the standard PD, respectively. An electrical vector network analyzer (EVNA, R&S ZVA67) provides the sweeping RF signal, PMD, and DSP. To extract the phase and magnitude information at the frequencies of $\omega_e \pm \Delta\omega$, an EVNA extension (Scalar Mixer and Harmonics, R&S ZVA-K4) is incorporated.

The standard PD is calibrated by an LCA (Agilent 86030A) to obtain its frequency response. After removing the frequency response of the standard PD, the frequency response of the phase modulator is successfully achieved by the proposed method, which is shown in Fig. 2. The frequency resolution is 2 MHz, which exhibits the fine structures of the responses. As a comparison, an OSA (Yokogawa AQ6370C) with a resolution of 0.02 nm is used to characterize the phase modulator. Due to the low power of the sidebands and poor resolution of the OSA, the modulated sidebands in the range of 0–10 GHz are overwhelmed by the carrier. Despite so, the measurement results of the proposed CVA fit the measurement results of the OSA very well in the range of 10–40 GHz, which verifies the effectiveness of the proposed CVA for E-O device measurement.

Figure 3 illustrates the frequency responses of the standard PD and the PD under test. According to the frequency responses of the standard PD and the phase modulator, the frequency responses of the PD under test are obtained. The frequency resolution is 2 MHz. As a comparison, the PD under test is also measured by an LCA. As can be seen, the measurement results of the CVA and LCA are quite similar. Furthermore, since the PD under test and the standard PD are of the same type, the frequency responses of the two PDs have similar trends.

Figure 4 exhibits the measured frequency responses of the sampled FBG by using the CVA. By removing the frequency response of the E-O and O-E devices, the frequency response of the O-O device is obtained. As a comparison, the sampled FBG is also measured by an OSA with a resolution of 0.02 nm cooperated with an amplified spontaneous emission (ASE) source (Amonics). The magnitude response measured by the CVA has a similar profile but exhibits a deeper notch, which indicates that the CVA has a larger dynamic range. The measurement range is 80 GHz, and the resolution is 2 MHz.

There are some issues to be noted. The resolution of this method depends mainly on the scanning step and the linewidth of the laser. By using a laser with an ultra-narrow linewidth and fine scanning, the resolution can be increased further. To obtain a stable and effective measurement, polarization controllers or polarization-maintaining fibers are used before the modulators. By adding a polarization controlling module [21] before the O-O devices, the polarization response can also be obtained.

In conclusion, the proposed CVA has the capability to measure the E-O, O-E, and O-O devices with arbitrary responses. The key problem of frequency aliasing, which makes it impossible for the commercial LCA to measure the phase modulator or O-O devices with frequency selectivity, is overcome by the proposed ADSB structure. A wideband PD (O-E device), a phase modulator (E-O device), and a sampled fiber Bragg grating (O-O device) are experimentally measured. The proposed ADSB-based CVA provides a compact, high-resolution, large dynamic range, and stable measurement approach for

characterizing E-O, O-E, and O-O devices with arbitrary responses.

Funding. National Key R&D Program of China (2018YFB2201803); Postgraduate Research & Practice Innovation Program of Jiangsu Province (KYCX18_0290).

Disclosures. The authors declare no conflicts of interest.

Data Availability. Data underlying the results presented in this paper are not publicly available at this time but may be obtained from the authors upon reasonable request.

REFERENCES

1. E. Wooten, K. Kissa, A. Yi-Yan, E. Murphy, D. Lafaw, P. Hallemeier, D. Maack, D. Attanasio, D. Fritz, G. McBrien, and D. Bossi, IEEE J. Sel. Top. Quantum Electron. **6**, 69 (2000).
2. J. Capmany and D. Novak, Nat. Photonics **1**, 319 (2007).
3. X. Zhang, H. Chi, X. Zhang, S. Zheng, X. Jin, and J. Yao, IEEE Microw. Wireless. Compon. Lett. **19**, 422 (2009).
4. P. D. Hale and D. F. Williams, IEEE Trans. Microw. Theory Tech. **51**, 1422 (2003).
5. P. Alto, *High-Speed Lightwave Component Analysis* (Agilent Technologies, 2000).
6. T. Qing, S. Li, M. Xue, and S. Pan, Opt. Lett. **41**, 3671 (2016).
7. Y. Shi, L. Yan, and A. E. Willner, J. Lightwave Technol. **21**, 2358 (2003).
8. E. H. Chan and R. A. Minasian, J. Lightwave Technol. **26**, 2882 (2008).
9. S. Zhang, H. Wang, X. Zou, Y. Zhang, R. Lu, and Y. Liu, Opt. Lett. **39**, 3504 (2014).
10. Y. Heng, M. Xue, W. Chen, S. Han, J. Liu, and S. Pan, IEEE Photonics Technol. Lett. **31**, 291 (2019).
11. T. Niemi, M. Uusimaa, and H. Ludvigsen, IEEE Photonics Technol. Lett. **13**, 1334 (2001).
12. D. K. Gifford, B. J. Soller, M. S. Wolfe, and M. E. Froggatt, Appl. Opt. **44**, 7282 (2005).
13. B. Guo, T. Gui, Z. Li, Y. Bao, X. Yi, J. Li, X. Feng, and S. Liu, Opt. Express **20**, 22079 (2012).
14. S. Pan and M. Xue, J. Lightwave Technol. **35**, 836 (2017).
15. O. Morozov, I. Nureev, A. Sakhabutdinov, A. Kuznetsov, G. Morozov, G. Il'in, S. Papazyan, A. Ivanov, and R. Ponomarev, Photonics **7**, 14 (2020).
16. S. P. Li, M. Xue, T. Qing, C. Y. Yu, L. G. Wu, and S. L. Pan, Opt. Lett. **44**, 3322 (2019).
17. T. Qing, S. Li, Z. Tang, B. Gao, and S. Pan, Nat. Commun. **10**, 5135 (2019).
18. T. Qing, M. Xue, M. H. Huang, and S. L. Pan, Opt. Lett. **39**, 6174 (2014).
19. T. Qing, S. Li, M. Xue, N. Zhu, and S. Pan, Opt. Express **25**, 4665 (2017).
20. M. G. Wang and J. P. Yao, IEEE Photonics Technol. Lett. **25**, 753 (2013).
21. M. Sagues and A. Loayssa, Electron. Lett. **47**, 47 (2011).